Residual Mechanical Properties of Fire-Damaged Concrete: NDT/DT Evaluation

Mohamed BAGHDADI [1] *, Mohamed Salah DIMIA [1], Ahmed Rafik BELAKHDAR [2]

[1] *LGC-ROI Laboratory, Civil Engineering Department, Faculty of Technology, Batna 2University, Batna, Algeria*
[2] *Mining Laboratory, Civil Engineering Department, Larbi Tebessi University, Tebessa, Algeria*

http://doi.org/10.5755/j02.ms.42441

Received 4August 2025; accepted 29 September 2025

Evaluating the residual mechanical properties of fire-damaged concrete is crucial for structural safety, yet the limitations of destructive testing (DT) have promoted the use of non-destructive tests (NDT), for effective in-situ assessment. This research explores the residual mechanical behavior of concrete and examines the predictive accuracy of NDT/DT in post-fire conditions. Concrete cylinders with consistent mix designs were subjected to temperatures ranging from 200 °C to 1000 °C, following a controlled natural fire curve applied via an electric furnace. After maintaining the target temperature for 90 minutes and allowing for natural cooling, DTs (compressive strength and stress-strength behavior) and NDTs (UPV and rebound hammer tests) were carried out. The static and dynamic elastic moduli were not directly tested but were derived using empirical correlations with UPV values. Temperature evolution inside the specimens was simulated using SAFIR software. The findings demonstrated a marked deterioration in mechanical performance beyond 400 °C, with compressive strength losses exceeding 80 % at 800 °C, both static and dynamic elastic moduli were reduced by nearly 98 %. Post-fire stress-strain behavior also indicated substantial losses in stiffness and ductility beyond 600 °C. UPV measurements correlated strongly with the decrease in residual strength. A regression model was developed to estimate residual compressive strength based on UPV results, validating the technique's relevance for post-fire assessments. The combined application of DT and NDT methods yielded a detailed understanding of thermal degradation. Notably, UPV demonstrated high sensitivity in detecting internal damage and estimating residual stiffness in fire damaged concrete. It thus offers engineers a reliable tool for evaluating whether repair or replacement is necessary, especially in contexts where DTs are not feasible.

Keywords: destructive testing, non-destructive testing, ultrasonic pulse velocity, residual mechanical properties.

1. INTRODUCTION

Concrete is the most widely used structural material in construction, owing to its strength, durability, and fire resistance. However, reinforced concrete structures are susceptible to extreme events such as earthquakes and fire accidents. During accidental fires, temperatures inside concrete members can exceed 1000 °C, depending on the duration and severity of exposure. These elevated temperatures induce changes in the physical and mechanical properties of concrete. After fire exposure, heat continues to penetrate the concrete cross-section during cooling, especially in large members, inducing thermal stress and delayed cracking [1, 2]. These phenomena often lead to additional internal damage, including microcracking and chemical alterations, such as the decomposition of calcium hydroxide, ultimately reducing strength. In addition to these changes, chemical analysis such as X-ray diffraction (XRD) can reveal alterations in the mineral composition, such as the decomposition of portlandite into calcium oxide at temperatures above 400 °C, as shown in recent studies [3 – 6]. However, this study focuses on mechanical aspects, with the suggestion to integrate XRD in future research to enhance understanding of chemical degradation.

Numerous studies [7 – 11] have investigated the effects of high temperatures on concrete and its residual mechanical properties (e.g., compressive and tensile strength and modulus of elasticity). Residual strength, measured after cooling, is generally lower than hot strength. Some investigations [12 – 18] have found that the minimum strength is reached once the concrete has returned to ambient temperature, emphasizing the importance of post-fire assessment.

Non-destructive tests (NDTs) are effective for detecting chemical and physical changes and damage in concrete. Among these, ultrasonic pulse velocity (UPV) is widely used to evaluate concrete quality by measuring the velocity of sound waves propagated through the material. Previous research has demonstrated that sound speed is sensitive to changes in compressive strength [19]. This is particularly evident in thermally damaged concrete, where UPV can detect deterioration caused by calcium silicate hydrate (C-S-H) gel dehydration, portlandite decomposition, and crack development, all of which impact material quality.

Another common NDT technique is the rebound hammer test, which assesses concrete strength based on surface hardness. The rebound of an elastic mass is directly proportional to surface hardness. When concrete is exposed to elevated temperatures, a decrease in surface hardness is expected because of reductions in density, moisture content, and overall mechanical properties. While various studies [4, 5, 20 – 25] have explored the use of destructive and non-destructive techniques, including compressive strength testing, rebound hammer, and UPV to characterize damage in fire-exposed concrete, the reliability of NDT methods in

*Correspondingauthor: M. Baghdadi
E-mail: *m.baghdadi@univ-batna2.dz*

detecting delayed failure or hidden degradation is debated. Nonetheless, NDT methods can provide a rapid and non-invasive assessment of post-fire structures, demonstrating the increasing importance of NDTs in guiding repair or demolition decisions.

Furthermore, several analytical and numerical models have been proposed to simulate the behavior of fire-damaged concrete [26 – 28]; however, most neglect the effects of the cooling phase. Therefore, there is a growing need for experimental data that reflect realistic fire exposure scenarios, including heating, stabilization, and natural cooling.

This study aims to provide a comprehensive assessment of the residual mechanical properties of concrete after exposure to fire, focusing on compressive strength and static and dynamic moduli of elasticity. To this end, cylindrical specimens (Ø160 mm × 320 mm) were exposed to controlled high temperatures up to 1000°C, following a natural fire curve with a heating rate of 3 – 8°C/min and a 90-minute plateau. After natural cooling, mechanical tests were conducted four months post-exposure. A 2D transient nonlinear thermal simulation was performed in parallel, using the SAFIR finite element software, to predict the internal temperature distribution. This dual experimental-numerical approach aims to fill the gap in current models by incorporating the full fire cycle, including the often-neglected cooling phase.

2. EXPERIMENTAL PROGRAM

The experimental methodology was designed to thoroughly investigate the post-fire behavior of concrete by evaluating compressive strength and static and dynamic moduli of elasticity at five target temperatures: 200, 400, 600, 800, and 1000 °C.

Uniaxial compression tests were conducted using a universal hydraulic press (Sematron, Besmak Co. Ltd.) with a maximum loading capacity of 1500 kN. The applied load was controlled and monitored through an integrated pressure transducer.

For the heating process, an electrically programmable furnace (Nabertherm) was used to expose the concrete specimens to the desired temperatures.

NDTs were performed using a Schmidt rebound hammer (Proceq) to determine the rebound number and a UPV device **(**Tico Proceq**)** to measure wave propagation through the specimens (Fig. 1).

2.1. Materials used

The raw materials used in the experiments are detailed below:

2.1.1. Cement

CEM I 42.5 R SR5 NA 442 was used. Table 1 presents the results of the Physico-mechanical properties and chemical analysis of the cement, performed using energy-dispersive spectrometry (EDS).

Table 1. Physico-mechanical properties and chemical composition of the CEM I cement

Chemical composition, %		Physical and mechanical properties	
CaO	62.22	Specific gravity, kg/dm^3	3.22
SiO_2	19.86		
Fe_2O_3	4.78	Specific surface, cm^2/g	3783
Al_2O_3	4.36		
Clinker C3A	4.35		
SO_3	2.86		
MgO	1.20	Compressive strength at the 28thday, MPa	42.5
Total composition	99.63		
Loss on Ignition (LOI)	2.51		
LOI value calculated according to the ignition method (mass loss upon heating at 1000 °C)			

2.1.2. Aggregates

Quarry sand was passed through a 3 mm sieve to obtain sand with a fineness modulus of 2.71, which was used as the fine aggregate. Crushed limestone was used as the coarse aggregate and was divided into two granulometric classes: 8/15 mm, particles ranging from 8 to 15 mm; 15/25 mm, particles ranging from 15 to 25 mm.

The particle size distributions of the sand and crushed limestone are shown in Fig. 2, and their main physical properties are summarized in Table 2.

a b c

Fig. 1. Test equipment and instrumentation: a – compression testing machine; b – Schmidt hammer and ultrasonic pulse velocity; c – programmable electrical furnace with integrated temperature controller

Table 2. Physical properties of coarse aggregates and sand

Property	Coarse aggregates 8/15	Coarse aggregates 15/25	Sand 0/3
Specific gravity	2.67	2.68	2.60
Unit weight, kg/dm^3	1.42	1.49	1.80
Los Angeles abrasion value, LA < 40	23 %	–	–
Flattening coefficient	14.27	8.91	–
Fine materials by volume , %	0.86	1.15	71(sand equivalent)
Water absorption, wt.%	1.2	1.1	1.2

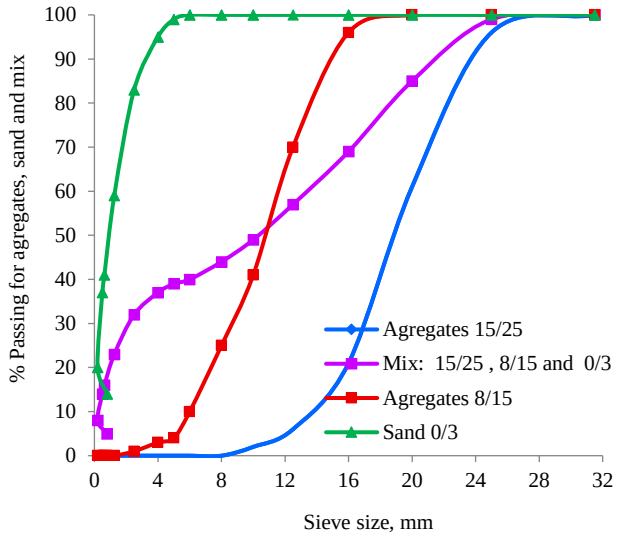

Fig. 2. Sieve analysis results for sand, coarse aggregates (8/15 and 15/25 mm), and their combined mix

2.1.3. Mixing water

Tap water supplied by the city was used for mixing and curing, following the XP P18-303 standard applicable to the prepared concrete mix.

2.2. Methods

2.2.1. Concrete mixing and composition

The concrete was designed using the Dreux-Gorisse method to achieve a C25/30 class compressive strength (25 – 30 MPa at 28 days), following NF EN 206/CN. A horizontal drum mixer was used, and workability was assessed using the Abrams cone per NF EN12350-2, yielding a slump of 70 mm, corresponding to consistency class S2 (50 – 90 mm). Concrete was poured into moulds in three layers, each compacted with a vibrating needle for ≥10 seconds. No bleeding or segregation was observed. The density of hardened concrete was 2354 kg/m^3.

All tests were performed on standard cylinders (Ø160 mm × 320 mm), complying with NF EN 12390-1/NA 2600/1992, using a binder content of 350 kg/m³ and a w/b ratio of 0.55. Table 3 lists the mix proportions [29]. The compressive strength reached 20 MPa at 7 days and 33 MPa at 28 days. Table 4 summarizes the mechanical properties.

2.2.2. Specimen casting and curing

Six cylindrical specimens (Ø160 mm × 320 mm) were cast per batch. After 24 hours, they were demoulded and cured in water at 20 ± 2 °C for 28 days in line with NF EN 12390-2(NA 5050).

Table 3. Mix composition of the tested concrete in kg/m³

Ingredients	Mix proportions for 1 m^3, kg
Cement (CEM I 42.5 R)	350
Coarse aggregate 15/25	728
Coarse aggregate (8/15+3/8)	448
Sand (quarry sand) 0/3	710
Water, L	193
Water-cement ratio	0.55
G/S ratio	1.65
Slump, mm	70

Table 4. Mechanical properties of concrete classified as C25/30

Compressive strength	fc_{28}	33 MPa
Tensile strength	Ft_{28}	0.0
Poisson's ratio	μ	0.2
Type of aggregates	Calcareous	–
Water content	w	4 %
Density of concrete	ρ	2354 kg/m^3

The specimens were then oven-dried at 110 °C for 72 hours**,** until a constant mass was obtained, thus eliminating free water and preventing explosive spalling at high temperatures. The final tests were conducted 120 days after fire exposure. The specimens had previously been cooled to room temperature (20 ± 2 °C) under ambient air conditions and stabilized at a relative humidity of 60 ± 10 % per NA 5050.

2.2.3. Thermal exposure protocol

Specimens were heated in a programmable electric furnace (maximum temperature is 1200 °C). The thermal cycle consisted of four phases [30]:

1. Heating phase: the temperature increased at a rate of 3 – 8 °C/min until the target temperature was obtained.
2. Stabilization phase: the target temperature was maintained for 90 minutes.
3. Cooling phase: controlled cooling inside the furnace at approximately 1 °C/min until room temperature was attained.
4. Post-fire phase: Specimens were stabilized at 20 ± 2 °C.Fig. 3 illustrates the furnace temperature-time evolution.

2.2.4. Testing procedure

Thirty-six cylinders were divided into six temperature groups: 20 °C (reference), 200, 400, 600, 800, and 1000 °C. Each group included 3 – 6 specimens, depending on the test. The following properties were measured before and after fire exposure: UPV, rebound number, static and dynamic moduli of elasticity, and compressive strength. Average values were used to represent each temperature. UPV and

surface hardness were measured at two stages (before and after exposure).

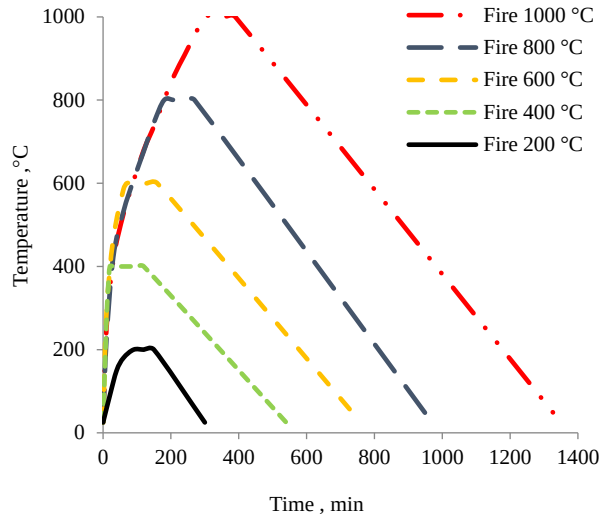

Fig. 3. Time-temperature evolution of the heating, stabilization, and cooling cycle

2.2.5. Temperature distribution in the cross-section of the concrete cylinders

Due to the complexity of measuring internal temperatures in concrete specimens, the temperature distribution across the cross-section of the concrete cylinders was assessed through 2D nonlinear transient thermal analyses, conducted using the SAFIR, finite element software developed at the University of Liège in Belgium [31].

Fig. 4a illustrates the temperature profile in a quarter-section (Ø16 cm) of the cylinders during fire exposure up to 1000 °C, showing a surface peak temperature of 998 °C at the end of the heating phase. During the cooling phase, the internal temperature remained higher than the surface temperature (Fig. 4b). For instance, under the 800 °C fire scenario, the core temperature (8 cm from the surface) reached 159 °C, while the surface dropped to 66 °C. This thermal gradient reversal may induce internal stress, delayed cracking, and residual deformations, even after cooling is complete.

3. RESULTS AND DISCUSSION

This section presents a comprehensive analysis of the results of the experimental study, focusing on the residual properties of fire-damaged concrete and the performance of NDTs. The compressive strength and static and dynamic moduli of elasticity data and UPV readings were thoroughly analyzed to fully understand the thermal impact. Variations in these properties were explored as a function of exposure temperature, the duration of the thermal plateau, and the cooling phase.

A comparative analysis was also conducted, contrasting the present observations with those from other relevant studies on the behavior of normal-strength concrete (NSC) exposed to elevated temperatures. This comparison aims to highlight similarities and discrepancies, thereby supporting the validity of the present results and contributing to a deeper understanding of thermal degradation mechanisms.

Finally, the effectiveness of NDTs, particularly UPV, is discussed in detail, evaluating their ability to accurately predict the residual properties of post-fire concrete.

3.1. Non-destructive tests (NDTs)

NDTs were employed to evaluate the physical condition and mechanical integrity of the concrete specimens before and after exposure to elevated temperatures, without alteringor damaging the samples. These methods are particularly valuable in post-fire assessments, where preserving the structural element is critical.

Two widely used NDTs were applied: UPV,which assesses internal deterioration and material homogeneity, and the rebound hammer test**,** which evaluates surface hardness and provides indirect insights into compressive strength. The following sections detail the implementation of these techniques, analyze their sensitivity to temperature induced damage, and discuss their correlation with destructive test (DT) results.

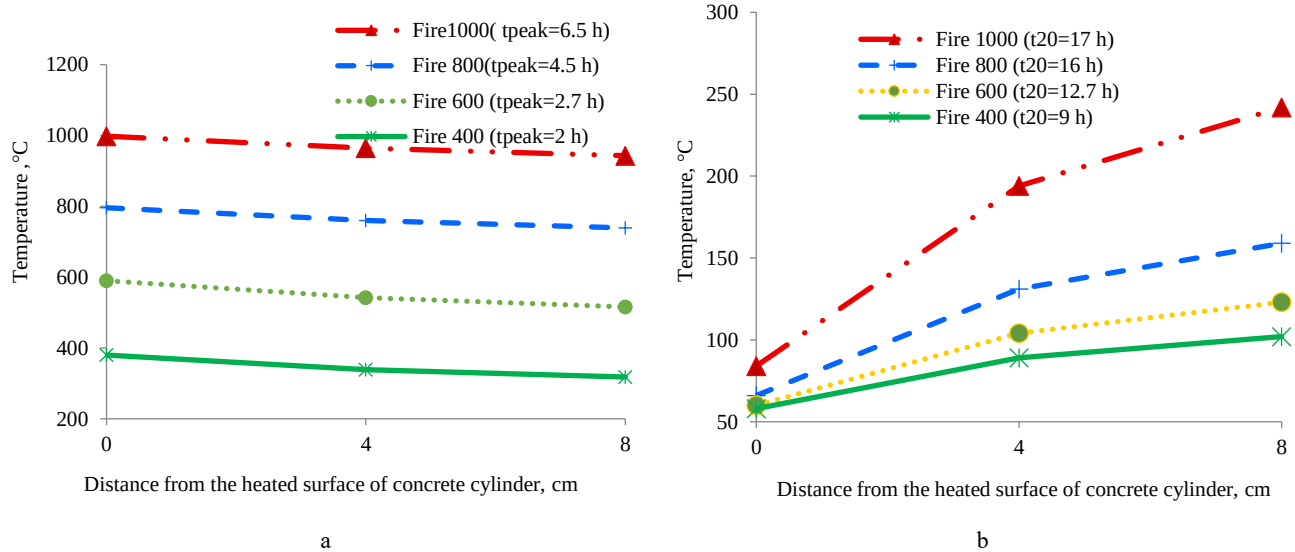

a b

Fig. 4. Temperature evolution across the concrete cylinder cross-section during heating and cooling

3.1.1. Surface hardness assessment by the rebound hammer test

The surface hardness of the concrete specimens was evaluated using a Schmidt rebound hammer, following the NA 2786 standard, which is technically identical to EN 12504-2(2001). For each specimen, the mean rebound number (R_n) was determined by averaging five measurements per face, with a 20 mm spacing between impact points.

This NDT is based on the principle that the rebound of an elastic mass is related to the hardness of the impacted surface, thereby reflecting the quality of the outer concrete layer up to a depth of approximately 30 mm. The results in Table 5 show a decrease in the rebound number after exposure to 600 °C and 800 °C, indicating a loss of surface hardness due to thermal degradation.

Table 5. Variation in the rebound number values (R_n) of concrete specimens

Specimen	Rebound number (R_n)		
	Before heating	After heating 600°C	After heating 800°C
Specimen 1	31	24	20
Specimen 2	32	25	20
Specimen 3	32	24	20
Specimen 4	31	23	20
Specimen 5	30	24	20

However, the reliability of this method for quantitative analysis is limited by its high sensitivity to multiple parameters, including cement type, aggregate properties, moisture content, surface carbonation, and the concrete age. Hence, no universal correlation exists between the rebound number and compressive strength. Nevertheless, the rebound test remains a practical tool for performing a qualitative evaluation of the surface condition of fire-exposed concrete [32].

3.1.2. Assessment of internal damage by ultrasonic pulse velocity (UPV)

The UPV method, compliant with EN 12504-4, was used to assess the internal integrity and extent of thermal damage in the concrete specimens. This NDT relies on the close relationship between the velocity of sound waves and the material's physical properties, including its elastic modulus, internal cohesion, and moisture content. Measuring the UPV (following NA 5027) allows estimating key residual performance indicators, such as the dynamic and static moduli of elasticity and compressive strength ($f_{c,r}$).

The progressive decrease in UPV with increasing temperature can be attributed to profound microstructural damage resulting from the decomposition of portlandite, the dehydration of the calcium-silicate-hydrate (C-S-H) gel, and microcracking caused by the thermal incompatibility between the cement paste and aggregates. This degradation is intensified by the successive loss of water in its various forms (free, capillary, and chemically bound), which alters the internal concrete structure and reduces wave velocity. Thus, UPV is particularly effective at detecting these heterogeneous internal damage zones caused by the steep thermal gradients within the concrete.

In addition to mechanical changes during the heating phase, the cooling phase can cause chemical reactions such as the rehydration of calcium oxide (CaO) into calcium hydroxide ($Ca(OH)_2$), which increases volumetric expansion and may result in delayed cracking. Studies using XRD have shown the disappearance of portlandite at high temperatures, with possible reformation during cooling (Colombo & Felicetti, 2007; Hager et al., 2020 and Wang et al., 2023) [20, 21, 24]. It is recommended to perform XRD analysis in future studies to confirm these chemical transformations.

This trend is quantitatively confirmed by the experimental results presented in Table 6 and Fig. 5.

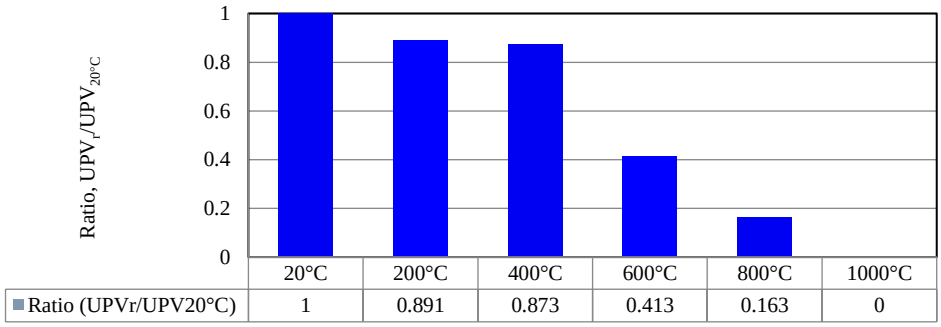

Fig. 5. Degradation of the $UPV_r/UPV_{20°C}$ ratio of unheated and heated concrete specimens

Table 6. Variation in the UPV values of unheated and heated concrete specimens

Velocity Specimens	UPV at 20°C, km/s	Mean value of UPV at 20°C, km/s	Temperature, °C	UPV after heating, km/s	UPV loss, %
Specimen 1	4.624	4.600	200	4.100	11.33
Specimen 2	4.590		400	4.020	12.41
Specimen 3	4.574		600	1.900	58.46
Specimen 4	4.644		800	0.750	84
Specimen 5	4.584		1000	–	–

Although the reference specimens exhibited high velocities (4.574 – 4.644 km/s), indicating good quality concrete, only a moderate decrease was observed at temperatures up to 400 °C. Beyond this threshold, there was a drastic drop in velocity, falling to 1.900 km/s at 600 C and just 0.750 km/s at 800 °C. At 1000 °C, the internal damage was so severe that wave propagation was no longer measurable. These findings confirm that UPV is a highly reliable indicator of thermal damage, especially when combined with mechanical property assessments for a comprehensive evaluation.

Table 7 shows values widely cited in literature. Whitehurst (1966) [19] pointed out that those values are based on normal concrete (≈ 2400 kg/m³) and that the boundaries between conditions are not clearly defined. Thus, he suggested comparing results with a known area of the structure for more reliable interpretation.

Table 7. Classification of concrete quality according to UPV [19]

Pulse velocity, km/s	Condition
Above 4.570	Excellent
3.660 to 4.570	Generallygood
3.050 to 3.660	Questionable
2.130 to 3.050	Generallypoor
Below 2.130	Verypoor

3.2. Residual mechanical properties of concrete determined by non-destructive and destructive tests

This section describes the residual mechanical properties of concrete after fire exposure. NDTs and DTs were performed for a comprehensive overview of the damage sustained by the material, both at the surface and internally. NDTs allow for an initial assessment of the damage, whereas DTs provide precise quantitative data on the remaining strength and stiffness of the concrete.

Among NDTs, UPV was used to evaluate internal degradation and calculate the static and dynamic moduli of elasticity, and the rebound hammer test was conducted to measure surface hardness. Among DTs, the uniaxial compressive strength and stress-strain behavior were measured.

The UPV test provided insights into the internal degradation of the concrete, allowing for an estimation of the dynamic modulus of elasticity (E_d), which decreased with rising temperature. Similarly, the static modulus of elasticity (E_s) was calculated based on empirical correlations with UPV values and validated through comparison with existing models from the literature (e.g. Mróz and Hager [22], EN 1994-1-2 [33]).

The rebound hammer test was used to assess changes in surface hardness, which are typically correlated with compressive strength. Destructive compressive strength tests were performed in accordance with NF EN 12390-3 on specimens before and after fire exposure.

3.2.1. Static modulus of elasticity determined by the UPV test

The static modulus of elasticity **($E_{s,r}$)** of concrete can be reliably estimated using the UPV test. This method leverages the strong correlation between the velocity of sound waves propagating through concrete (V in km/s) and its stiffness. Mróz and Hager [22] support this approach, having developed a power-law regression modelgiven by Formula 1 that accurately predicts $E_{s,r}$ for various types of concrete, irrespective of their composition. In addition to derivation from UPV method, it is recommended to measure $E_{s,r}$ directly using strain gauges during compression tests to validate the empirical relationships, especially in fire-damaged concrete, where properties may vary unpredictably [5]. The present analysis was based on an empirical relationship; however, the results exhibited agreement with data reported in the literature, thereby supporting the validity of this approach.

$$E_{s,r} = 988(V)^{2.33}. \quad (1)$$

The $E_{s,r}$ values predicted by the model of [22] were consistent with analytical formulations proposed by Eurocode EN 1994-1-2 [33] and Chang et al. [27] (Eq. 4 and Eq. 5) (see Table 8 and Fig. 6). The equations governing this relationship are given below:

$$\frac{E_{s,r}}{E_{s,20}} = \begin{cases} -0.00165T + 1.033\ ;\ 20°C < T \le 125°C \\ \frac{1}{1.2+18(0.0015T)^{4.5}}\ ;\ 125°C \le T \le 800°C \end{cases}; \quad (2)$$

$$\frac{E_{s,r}}{E_{s,20}} = 0.00165T + 1.033;\ 20°C < T \le 600°C \quad . \quad (3)$$

These findings consistently show a marked drop in the static modulus of elasticity as temperature increases, indicating progressive deterioration of the internal structure of concrete.

3.2.2. Dynamic modulus of elasticity determined by the UPV test

The dynamic modulus of elasticity **(E_d)** of concrete was determined by ultrasonic pulse transmission through the specimens, applying Eq. 2, proposed by Torić et al.[15].

The suggested relationship can be expressed as Eq. 4:

$$E_{d,r} = \frac{V^2.\rho(1+\mu_d)(1-2\mu_d)}{(1-\mu_d)}. \quad (4)$$

This equation links wave speed (V) in km/s,ρ (concrete density in kg/m³), and μ_d (Poisson's ratio = 0.2).

Table 8. Residual mean $E_{s,r}$ values of unheated and heated concrete specimens (the experimental results were obtained using Eq. 1, proposed by [22], and were compared with other studies)

Temperature, °C	V, km/s	$E_{s,r}/E_{s,20°}$experimental results by [22]	$E_{s,r}/E_{s,20°}$[33]	$E_{s,r}/E_{s,20°}$from Eq. 4 [27]	$E_{s,r}/E_{s,20°}$fromEq. 5 [27]
20	4.600	1	1	1	1
200	4.050	0.74	0.40	0.78	0.70
400	3.250	0.44	0.17	0.33	0.37
600	1.900	0.12	0.06	0.08	0.043
800	0.750	0.014	0.035	0.05	–

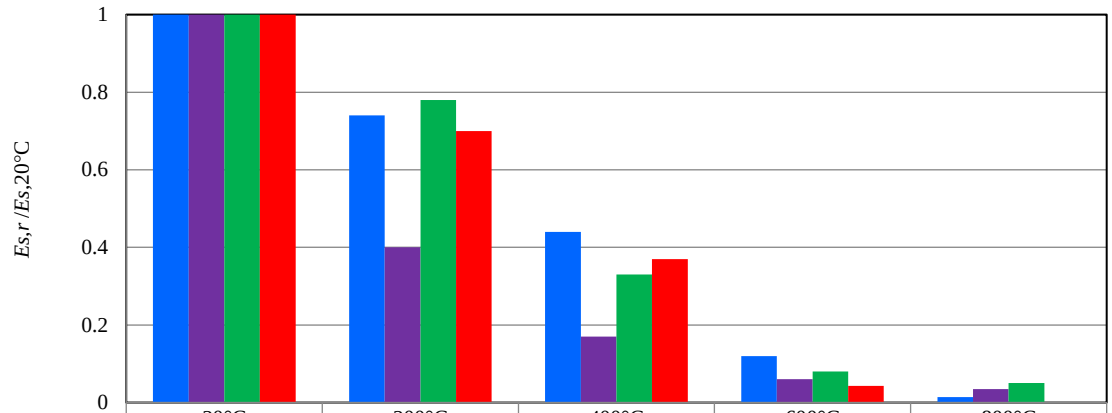

	20°C	200°C	400°C	600°C	800°C
Experimenal results	1	0.74	0.44	0.12	0.014
EN1994 1-2	1	0.4	0.17	0.06	0.035
Eq(4) Chang et al	1	0.78	0.33	0.08	0.05
Eq(5) Chang et al	1	0.7	0.37	0.043	

Fig. 6. Degradation of $E_{s,r}/E_{s,20^\circ}$ of the concrete specimens after fire exposure

For the analytical evaluation, Poisson's ratio was fixed at 0.2, following recommendations in [15]. This value is commonly assumed for fire-damaged concrete in analytical models [26, 27]. The constant value provides a reasonable approximation for UPV-based calculations and aligns with international fire design standards [35].

The experimental results (Table 9, Fig. 7) showed good agreement with EN 1994-1-2 [33] and with data from Dvořák and Chobola [5].

Table 9. $E_{d,r}$ reduction in unheated and heated concrete specimens (the experimental results were obtained using Eq. 4, proposed by [15], and compared with other studies)

Temperature, °C	Mean value of V, km/s	$E_{d,r}/E_{d,20^\circ}$experimental results	$E_{d,r}/E_{d,20^\circ}$from [5]	$E_{d,r}/E_{d,20^\circ}$ from[33]
20	4.600	1	1	1
200	4.050	0.77	0.82	0.45
400	3.250	0.50	0.65	0.22
600	1.900	0.17	0.32	0.08
800	0.750	0.02	0.09	–
1000	–	–	0.022	–
1200	–	–	0.07	–

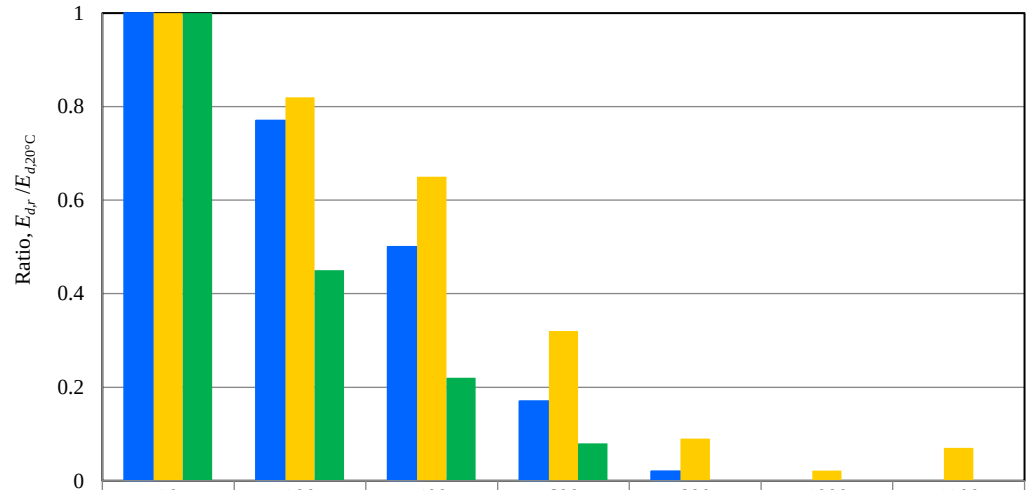

	20	200	400	600	800	1000	1200
Experimental resutls	1	0.77	0.5	0.17	0.02		
Eq Dvořák et Chobola	1	0.82	0.65	0.32	0.09	0.022	0.07
EN 1994-1-2	1	0.45	0.22	0.08			

Fig. 7. Degradation of the $E_{d,r}/E_{d,20^\circ}$ ratio in unheated and heated concrete specimens

The dynamic modulus of the unheated reference concrete reached 44 GPa. A progressive decline in ($E_{d,r}$) was observed with increasing temperature. The most substantial reduction occurred between 400 °C and 600 °C, where the modulus fell sharply from 29 GPa to 14 GPa. The decline continued beyond 600 °C, reaching a minimum of 01 GPa at 1000 °C. At this extreme temperature, the specimens showed the most severe degradation of their physical and mechanical properties.

These findings are consistent with destructive compressive strength tests (Table 10), confirming that (E_d)is a reliable indicator of temperature-induced damage in concrete.

3.2.3. Compressive strength

3.2.3.1. Destructive test

After fire exposure, the concrete cylinders were allowed to cool to ambient temperature and were subsequently tested by compression per the NF EN 12390-3 standard. The experimental results (Table 10 and Fig. 8) revealed a progressive loss of compressive strength with increasing temperature:

1. at 200 °C, the strength decreased by approximately 17.4%**,** primarily due to the evaporation of free water;
2. at 400 °C, the reduction reached 26 %, associated with total moisture loss and the onset of microstructural degradation;
3. at 600 °C and 800 °C, the strength dropped sharply to 63 % and 85 %, respectively;
4. at 1000 °C, the specimens were completely disintegrated and could not be tested.

This degradation can be attributed to a combination of thermally induced phenomena, including progressive loss of physically and chemically bound water, decomposition of calcium silicate hydrate (C–S–H) gel, and the breakdown of calcium hydroxide ($Ca(OH)_2$), especially beyond 400 °C [34].

The experimental findings were compared with analytical models and standards, including EN 1994-1-2 [33], EN 1992-1-2 [35], Li and Franssen's results [28], and Chang et al.'s model [27] (Eq. 1 and Eq. 2). The empirical relationships are given by the following two equations:

$$\frac{f_{c,T}(T)}{f_{c,20}} = 1.008 + \frac{\mathrm{T}}{450\ln\left(\frac{\mathrm{T}}{5800}\right)} \geq 0.0, \quad 200°C < T \leq 800°C; \tag{5}$$

$$\frac{f_{c,T}(T)}{f_{c,20}} = \begin{cases} 1.01 - 0.00055T; 20°C < T \leq 200°C \\ 1.15 - 0.00125T; 200°C \leq T \leq 800°C \end{cases}. \tag{6}$$

A good agreement was observed with Chang et al.'s model [27], particularly at temperatures up to 400 °C. However, beyond this threshold, the experimental results exhibited additional strength losses during and after the cooling phase, effects that are not fully accounted for in the Eurocode-based models.

Notably, post-cooling losses can reach up to 20 % of the initial strength, exceeding the 10 % residual loss estimated by EN 1994-1-2[33], particularly around 400°C.

3.2.3.2. Rebound hammer test

The compressive strength of concrete was estimated using the rebound hammer method, following EN 12504-2. The average rebound index (R_n) was calculated and used to estimate the compressive strength of concrete ($f_{c,Rn}$).

The correlation between the rebound index and compressive strength is derived from the empirical relation proposed by [36], and is given by Eq. 7:

$$f_{c,Rn} = \frac{R_n^2}{32}, \tag{7}$$

where $f_{c,Rn}$ is the estimated compressive strength in MPa;R_n is the average rebound value, measured using a Schmidt rebound hammer.

Table 11 presents the measured compressive strength of the specimens. Fig. 9 presents a comparison of the compressive strength measured by NDTs and DTs.

Table 10. Reduction in the mean residual compressive strength ($f_{c,r}$) of unheated and heated concrete specimens

Mean value of $f_{c,20°C}$, MPa	Temperature, °C	Experimental results $f_{c,r}$, MPa	Test result$f_{c,r}/f_{c,20°C}$, %	$f_{c,r}$loss, %
33.05	200	27.28	82.54	17.46
	400	24.42	73.88	26.12
	600	12.29	37.18	62.82
	800	4.98	15.07	84.93

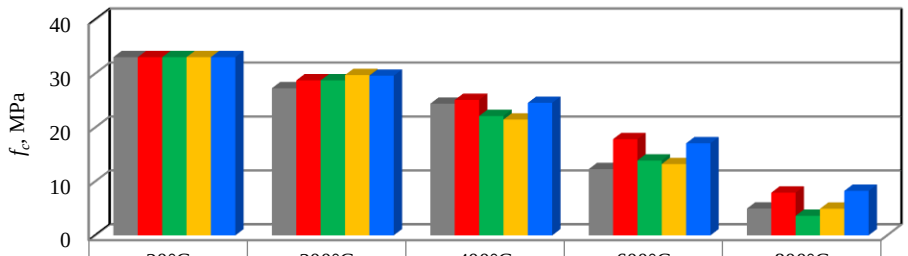

	20°C	200°C	400°C	600°C	800°C
Experimental result	33.05	27.28	24.42	12.29	4.98
EN 1994-1-2	33.05	28.75	25.12	17.84	7.93
Eq(1)Chang	33.05	28.75	22.14	13.88	3.63
Eq (2) Chang	33.05	29.74	21.48	13.22	4.95
Li and Franssen	33.05	29.61	24.58	17.08	8.26

Fig. 8. Degradation of residual compressive strength ($f_{c,r}$) of unheated and heated concrete specimens compared to published results

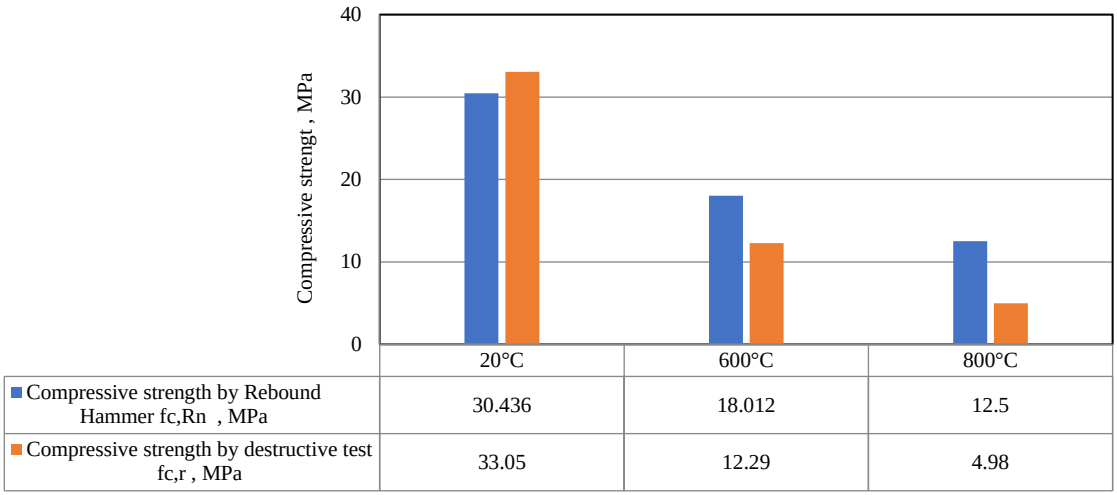

Fig. 9. Compressive strength measured via the rebound test and destructive test of unheated and heated concrete specimens

These results confirm the limited reliability of rebound hammer tests for quantitative post-fire assessment, in line with previous observations.

Table 11. Estimated compressive strength of unheated and heated concrete specimens, measured using a Schmidt rebound hammer $f_{c,Rn}$, MPa

Specimens	At 20°C	After heating 600°C	After heating 800°C
Specimen1	30.03	18.00	12.50
Specimen 2	32.00	19.53	12.50
Specimen 3	32.00	18.00	12.50
Specimen 4	30.03	16.53	12.50
Specimen 5	28.12	18.00	12.50

3.2.4. Correlation between residual compressive strength and ultrasonic pulse velocity in fire-exposed concrete

NDTs represent a reliable approach for monitoring newly built structures and assessing the extent of damage in existing ones. UPV testing is widely used to investigate the relationship between concrete quality and compressive strength because the ultrasonic wave velocity is influenced by the material's density and internal integrity, both of which correlate with its mechanical performance.

Fig. 10 and Fig. 11 provide a comparative analysis of compressive strength and UPV measurements for concrete specimens exposed to increasing temperatures. The UPV values progressively declined, reflecting the reduction in compressive strength. As shown in Fig. 10, both parameters decrease linearly with temperature, following their respective regression Eq. 8 and Eq. 9:

$$f_{c,r} = -0.036x + 35.09\ ;\ R^2=0.963; \quad (8)$$

$$UPV_r = -5.072x + 5123\ ;\ R^2=0.894. \quad (9)$$

Fig. 11 illustrates the degradation trend, using normalized values. The ratios of residual compressive strength $f_{c,r}/f_{c,20°C}$ and UPV ($UPV_r/UPV_{20°C}$) are shown.

These ratios also follow a linear trend with temperature, following their respective regression Eq. 10 and Eq. 11:

$$\frac{f_{c,r}}{f_{c,20°C}} = -0.001x + 1.074\ ;\ R^2=0.981; \quad (10)$$

$$\frac{UPV_r}{UPV_{20°C}} = -0.001x + 1.059\ ;\ R^2=0.962. \quad (11)$$

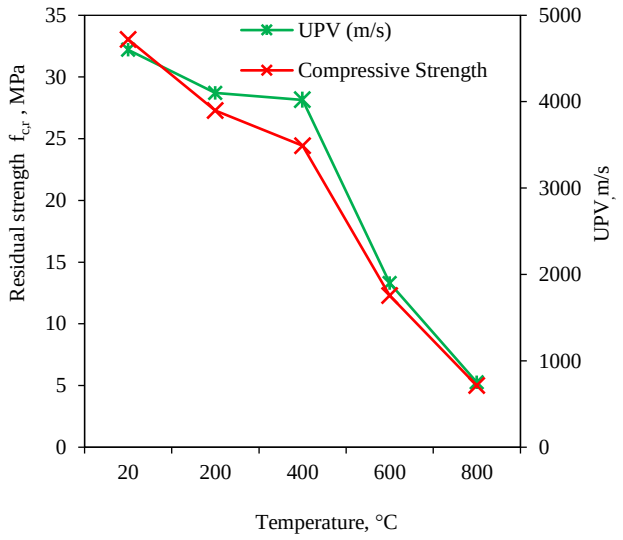

Fig. 10. Residual compressive strength (y = -0.036x + 35.09 with R^2 = 0.963) and UPV (y = -5.072x + 5123 with R^2 = 0.894) results of the concrete specimens

These strong correlations confirm that UPV is effective for evaluating the residual compressive strength of fire-exposed concrete. The close agreement between the results of DTs and NDTs validates UPV as a predictive tool.

Based on these findings, a linear predictive model was proposed (Fig. 12) to estimate residual compressive strength from UPV measurements.

Fig. 12 illustrates the correlation between the residual compressive strength ratio and UPV ratio of concrete subjected to various temperatures. The relationship between these two ratios exhibits a nearly linear trend along the first bisectrix, suggesting direct proportionality.

Accordingly, the following regression Eq. 12 is proposed to describe the dependency between the results of the two tests:

$$R_{fc} = 0.985.R_{UPV} + 0.0232, \quad (11)$$

where

$$R_{fc} = \frac{f_{c,r}}{f_{c,20°C}} \text{ and } R_{UPV} = \frac{\text{UPV}_\text{r}}{\text{UPV}_{20°\text{C}}}. \quad (12)$$

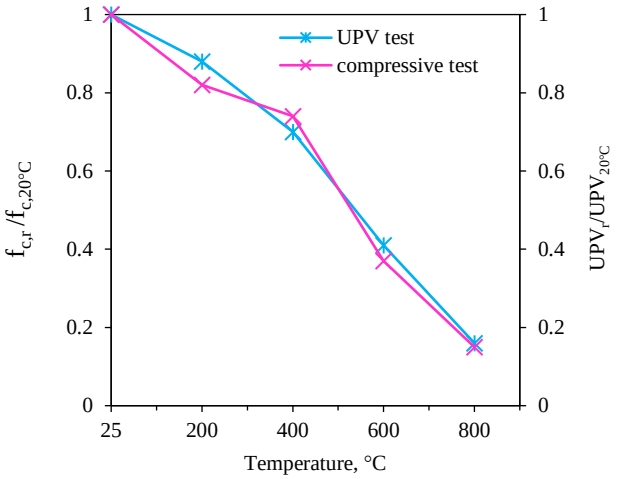

Fig. 11. Ratios of residual strength (y = -0.001x + 1.074 with R^2 = 0.981) and UPV (y = -0.001x + 1.059 with R^2 = 0.962) of the concrete specimens

The data indicate a strong positive correlation between the residual compressive strength ratio and the UPV ratio, with a coefficient of determination of R^2 = 0.987.

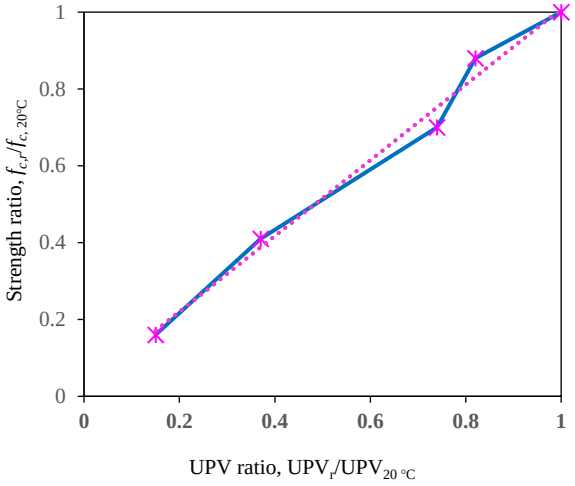

Fig. 12. Correlation of concrete compressive strength with UPV. A strong positive correlation was observed (R^2 = 0.987)

Eq. 12 indicates a direct linear relationship between the residual compressive strength and the residual UPV, both expressed as ratios relative to their initial values at ambient temperature. It suggests that the loss in compressive strength due to fire exposure can be reliably estimated from the corresponding reduction in UPV. For a given concrete composition, a decrease in wave velocity is therefore indicative of a proportional reduction in load-bearing capacity.

This correlation confirms the relevance of UPV as an effective NDT for assessing the mechanical condition of fire-damaged concrete, especially in situations where destructive testing is not feasible or permitted.

3.3. Post-fire stress-strain curves

The stress-strain behavior of concrete after fire exposure serves as a key indicator of the extent of thermal degradation. Increasing peak temperatures, particularly at 600 °C and 800 °C, led to more monotonic stress-strain curves (Fig. 13), indicating a marked reduction in stiffness and ductility. This observation reflects the diminished ability of the material to resist deformation and absorb energy before failure.

Specimens subjected to these elevated temperatures exhibited notable reductions in peak stress and strain capacity, confirming severe mechanical degradation. These changes are primarily influenced by the maximum temperature reached during heating, rather than by residual thermal effects after cooling.

The degradation mechanisms include a weakening of the bond between aggregates and the cement matrix, the formation of microcracks due to thermal gradients and shrinkage during cooling, and differential thermal contraction among the material's constituents, exacerbating internal damage.

Overall, the post-fire stress-strain response is a reliable indicator of internal deterioration in concrete exposed to elevated temperatures, underscoring the critical impact of thermal exposure on the structural performance of concrete elements.

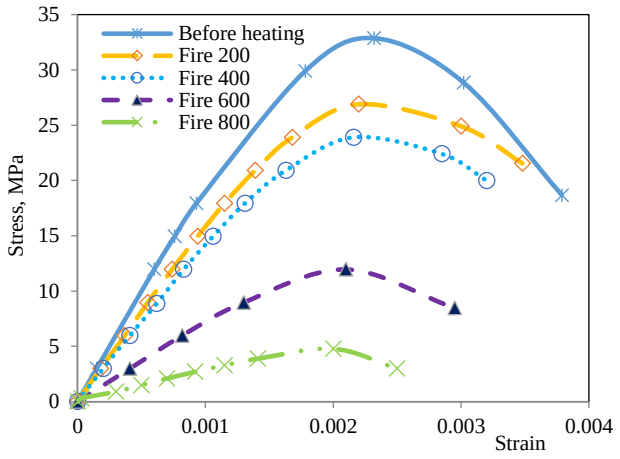

Fig. 13. Post-fire stress-strain curves of concrete after heating at different temperatures

4. FUTURE RESEARCH DIRECTIONS

Although our findings confirm the effectiveness of UPV for post-fire assessment, some limitations should be acknowledged. This study was based on standard cylindrical specimens tested under controlled laboratory conditions. However, in real structures, factors such as reinforcement, boundary constraints, variable heating exposure, and load conditions during fire may influence residual properties. Furthermore, static and dynamic elastic moduli were derived from empirical models without direct validation through physical measurements.

Therefore, future work should focus on: full-scale testing of reinforced structural elements; direct *in-situ* measurements of dynamic and static moduli; application of combined NDT techniques (e.g. UPV + infrared

thermography); incorporation of machine learning for automated damage classification based on UPV data; conduct chemical analyses such as X-ray diffraction (XRD) to confirm changes in mineral composition during all fire duration including cooling phase, such as the decomposition of portlandite and C–S–H, as demonstrated in recent studies [4, 25]. This will allow for a deeper understanding of chemical degradation mechanisms during cooling.

5. CONCLUSIONS

This study presents a detailed investigation of the residual mechanical properties of normal-strength concrete after fire exposure. Cylindrical specimens were subjected to various heating-cooling regimes, ranging from 200 °C to 1000 °C. Mechanical performance was evaluated using uniaxial compression tests, rebound hammer measurements, and ultrasonic pulse velocity (UPV) testing.

Despite the effectiveness of UPV, the study is limited by the absence of chemical analysis such as XRD, which could confirm mineral changes resulting from fire exposure. In the future, integrating these techniques is recommended for a more comprehensive assessment.

The experimental results revealed progressive and marked degradation. Compressive strength decreased by 17.4 % at 200 °C and 26 % at 400 °C, with sharper losses at higher temperatures: 63 % at 600 °C and 85 % at 800 °C. At 800 °C, both static and dynamic elastic moduli were reduced by nearly 98 %. Post-fire stress-strain behavior also indicated substantial losses in stiffness and ductility beyond 600 °C, linked to internal micro-structural damage and the breakdown of cement matrix cohesion.

UPV showed a strong correlation with these mechanical losses. At 600 °C and 800 °C, ultrasonic velocity decreased by 58.5 % and 84 %, respectively, and became unmeasurable at 1000 °C. A regression equation was proposed to express the relationship between compressive strength and UPV values, confirming UPV's viability for internal damage detection.

In summary, the combined use of destructive and non-destructive testing provided a reliable framework for evaluating fire-induced damage in concrete. UPV, in particular, can be considered a robust and scalable technique for structural assessment, especially when destructive methods are limited.

REFERENCES

1. **Baghdadi, M., Dimia, M.S., Baghdadi, D.** A Parametric Study of Fire-Damaged Reinforced Concrete Columns under Lateral Loads *Engineering, Technology & Applied Science Research* 12 (5) 2022: pp. 9113 – 9119. https://doi.org/10.48084/etasr.5172
2. **Takla, M., Tarsha, I.** Effect of Temperature on Carrying Capacity of Concrete Columns Confined with Multi-layers of CFRP *Jordan Journal of Civil Engineering* 14 (1) 2020: pp. 14 – 26.
3. **Hager, I.** Behaviour of Cement Concrete at HighTemperature *Bulletin of the Polish Academy of Sciences Technical Sciences* 61 (1) 2013: pp. 145 – 154. https://doi.org/10.2478/bpasts-2013-0013
4. **Krzemień, K., Hager, I.** Post-Fire Assessment of Mechanical Properties of Concrete with the Use of the Impact-Echo Method *Construction and Building Materials* 96 2015: pp. 155 – 163. https://doi.org/10.1016/j.conbuildmat.2015.08.007
5. **Dvořák, R., Chobola, Z.** Non-Destructive Testing and X-Ray Diffraction Analysis of High-temperature Degraded Concrete *Civil Engineering Journal* 27 (03) 2018: pp. 268 – 275. https://doi.org/10.14311/CEJ.2018.03.0022
6. **Heap, M.J., Lavallee, Y., Laumann, A., Hess, K.U., Meredith, P.G., Dingwell, D.B., Huismann, S., Weise, F.** The Influence of Thermal-Stressing (up to 1000°C) on the Physical, Mechanical, and Chemical Properties of Siliceous-Aggregate, High-Strength Concrete *Construction and Building Materials* 42 2013: pp. 248 – 265. https://doi.org/10.1016/j.conbuildmat.2013.01.020
7. **Sancak, E., Sari, Y.D., Simsek, O.** Effects of Elevated Temperature on Compressive Strength and Weight Loss of the Light-Weight Concrete with Silica Fume and Superplasticizer *Cement and Concrete Composites* 30 (8) 2008: pp. 715 – 721. https://doi.org/10.1016/j.cemconcomp.2008.01.004
8. **Lee, J., Xi, Y., Willam, K.** Properties of Concrete after High-Temperature Heating and Cooling *ACI Materials Journal* 105 (4) 2008: pp. 334 – 341. https://doi.org/10.14359/19894
9. **Shaikh, F.U.A., Taweel, M.** Compressive Strength and Failure Behaviour of Fibre Reinforced Concrete at Elevated Temperatures *Advances in Concrete Construction* 3 (4) 2015: pp. 283 – 293. https://doi.org/10.12989/acc.2015.3.4.283
10. **Anunai, R., Siempu, R.** Behavior of High Strength Concrete Subjected to Elevated Temperature *International Journal of Innovative Technology and Exploring Engineering* 9 (2) 2019: pp. 2997 – 3000. https://doi.org/10.35940/ijitee.B8028.129219
11. **Alhamad, A., Yehia, S., Lublóy, É., Elchalakani, M.** Performance of Different Concrete Types Exposed to Elevated Temperatures: A Review *Materials* 15 (14) 2022: pp. 5032. https://doi.org/10.3390/ma15145032
12. **Wisal, A., Lim, C.W., Arslan, A.** Influence of Elevated Temperatures on the Mechanical Performance of Sustainable-Fiber-Reinforced Recycled Aggregate Concrete: A Review *Buildings* 12 (4) 2022: pp. 487. https://doi.org/10.3390/buildings12040487
13. **Xiao, J., Falkner, H.** On Residual Strength of High-Performance Concrete with and Without Polypropylene Fibres at Elevated Temperatures *Fire Safety Journal* 41 (2) 2006: pp. 115 – 121. https://doi.org/10.1016/j.firesaf.2005.11.004
14. **Klingsch, E., Frangi, A., Fontana, M.** Experimental Analysis of Concrete Strength at High Temperatures and after Cooling *Journal of Advanced Engineering* 9 (1) 2009: pp. 34 – 38. https://doi.org/10.14311/1087
15. **Torić, N., Boko, I., Peroš, B.** Reduction of Post fire Properties of High-Strength Concrete *Advances in Materials Science and Engineering* 4 2013: pp. 1 – 9. https://doi.org/10.1155/2013/712953
16. **Kim, Y., Lee, T., Kim, G.** An Experimental Study on the Residual Mechanical Properties of Fiber Reinforced Concrete with High Temperature and Load *Materials and Structures* 46 (4) 2013: pp. 607 – 620. https://doi.org/10.1617/s11527-012-9918-y
17. **Torić, N., Boko, I., Juradin, S., Baloević, G.** Mechanical Properties of Light-Weight Concrete after Fire Exposure *Structural Concrete Journal* 17 (6) 2016: pp. 1071 – 1081. https://doi.org/10.1002/suco.201500145

18. **Elsanadedy, H.M.** Residual Compressive Strength of High-Strength Concrete Exposed to Elevated Temperatures *Advances in Materials Science and Engineering* 4 2019: pp. 1 – 22. https://doi.org/10.1155/2019/6039571
19. **Whitehurst, E.A.** Evaluation of Concrete Properties from Sonic Tests. American Concrete Institute (ACI)monograph 2, ACT, Detroit (Michigan, USA)1966: pp. 94. https://lib.ugent.be/catalog/rug01:001031912
20. **Colombo, M., Felicetti, R.** New Non-Destructive Techniques for the Assessment of Fire-Damaged Concrete Structures *Fire Safety Journal* 42 (6 – 7) 2007: pp. 461 – 472. https://doi.org/10.1016/j.firesaf.2006.09.002
21. **Hager, I., Carré, H., Krzemień, K.** Damage Assessment of Concrete Subjected to High Temperature by Means of the Ultrasonic Pulse Velocity – UPV Method *Studies and Researches* 32 2013: pp. 197 – 211.

    Mróz, K., Hager, I. Non-Destructive Assessment of Residual Strength of Thermally Damaged Concrete Made with Different Aggregate Types *Proceedings of the IOP Conference Series: Materials Science and Engineering* 2017: pp. 1 – 8. https://doi.org/10.14311/CEJ.2018.03.0022
22. **Wróblewski, R., Stawiski, B.** Ultrasonic Assessment of the Concrete Residual Strength after a Real Fire Exposure *Buildings* 10 (9) 2020: pp. 154. https://doi.org/ 10.3390/buildings10090154
23. **Wang, Y., Cui, J., Deng, J., Zhou, H.** Experimental Study of Thermally Damaged Concrete under a Hygrothermal Environment by Using a Combined Infrared Thermal Imaging and Ultrasonic Pulse Velocity Method *Materials* 16 (3) 2023: pp. 1040. https://doi.org/10.3390/ma16031040
24. **Gong, J., Deng, G., Shan, B.** Performance Evaluation of RPC Exposed to High Temperature Combining Ultrasonic Test: A Case Study *Construction and Building Materials* 157 2017: pp. 194 – 202. https://doi.org/10.1016/j.conbuildmat.2017.08.140
25. **Li, L.Y., Purkiss, J.** Stress–Strain Constitutive Equations of Concrete Material at Elevated Temperatures *Fire Safety Journal* 40 (7) 2005: pp.669 – 686. https://doi.org/10.1016/j.firesaf.2005.06.003
26. **Chang, Y.F., Chen, Y.H., Sheu, M.S., George, C.Y.** Residual Stress–Strain Relationship for Concrete after Exposure to High Temperatures *Cement and Concrete Research* 36 (10) 2006: pp. 1999 – 2005. https://doi.org/10.1016/j.cemconres.2006.05.029
27. **Li, H.Y., Franssen, J.M.** Test Results and Model for the Residual Compressive Strength of Concrete after a Fire *Journal of Structural Fire Engineering* 2 (1) 2011: pp. 29 – 44. https://doi.org/10.1260/2040-2317.2.1.29
28. **Baghdadi, M., Dimia, M.S., Guergah, C., Rabehi, R., Belakhdar, A.R.** Experimental and Numerical Investigation on the Behavior and Strengthening of Fire-Damaged Reinforced Concrete Walls Using Self-Compacting Concrete Jacketing *Materials Science (Medžiagotyra)* 2025: pp. 1 – 10. http://doi.org/10.5755/j02.ms.41042
29. **Baghdadi, M., Dimia, M.S., Guenfoud, M., Bouchair, A.** An Experimental and Numerical Analysis of Concrete Walls Exposed to Fire *Structural Engineering and Mechanics* 77 (6) 2021: pp. 819 – 830. http://doi.org/10.12989/SEM.2021.77.6.819
30. **Franssen, J.M., Gernay, T.** Modeling Structures in Fire with SAFIR: Theoretical Background and Capabilities *Journal of Structural Fire Engineering* 8 (3) 2017: pp. 300 – 323. http://doi.org/10.1108/JSFE-07-2016-0010
31. **Bungey, J.H., Millard, S.G.** Testing of Concrete in Structures 3rd edition Blackie Academic and Professional 1996: pp. 286. http://worldcat.org/isbn/0751402419
32. **European Committee for Standardization**. EN 1994-1-2 (Eurocode 4) Design of Composite Steel and Concrete Structures. Part 1 – 2: General rules – Structural fire design Brussels 2005.
33. **Kalifa, P., Chene, G., Galle, C.** High-Temperature Behaviour of HPC with Polypropylene Fibres: From Spalling to Microstructure *Cement and Concrete Research* 31 (10) 2001: pp. 1487 – 1499. https://doi.org/10.1016/S0008-8846(01)00596-8
34. **European Committee for Standardization.** EN 1992-1-2 (Eurocode 2) Design of Concrete Structures – Part 1 –-2: General rules – Structural fire design Brussels 2004.
35. **Dupain, R., Arroman, J.C.S.** Granulats, Sols, Ciment et bétons 4th edition CASTEILLA 2009: pp. 286.